Second International Dam World Conference
PORTUGAL • LISBON • LNEC • April 21-24, 2015

THERMAL ANALYSIS OF CONCRETE DAMS DURING CONSTRUCTION PHASE

Eloísa M. Castilho[†], Noemi Schclar Leitão* and Carlos Tiago[‡]

*Laboratório Nacional de Engenharia Civil (LNEC)
Av. do Brasil, 101, 1700-066 Lisboa, Portugal
e-mail: nschclar@lnec.pt

Keywords: Heat of hydration, Concrete, Finite elements, Thermo-chemical analysis

Abstract. *This paper reports a case study of the thermal analysis of a concrete dam during its construction phase. The thermo-chemical problem is solved using a heat transfer model. In the absence of specific adiabatic calorimetric tests of the concrete, an exponential function was calibrated by the best fitting of estimated heat of hydration at the ages of 3, 7 and 28 days. The predicted temperatures obtained from the code are compared with the actual temperatures measured in situ by the monitoring system installed in the dam.*

1 INTRODUCTION

Heat generated by the hydration of cement produces high temperature which does not quickly dissipate. The surface of the dam cools faster than its interior. This causes a temperature gradient between the cooled surface and the hot interior mass. Such a difference will result in a thermal gradient that is likely to generate undesirable thermal stresses which may cause cracks at the exterior surface. So, thermal analysis should be performed for mass concrete dams to provide a basis to minimize and control the occurrence of thermal cracking[1].

Several techniques have been reported in the literature to evaluate the thermal performance of concrete structures during the hydration phase. These techniques range from complex three-dimensional numerical models to simple manual computation. In one hand, multiscale formulations have been proposed, coupling a cement hydration model on the microscale with the finite element method heat conduction problem on the macroscale[2]. On the other hand, the ACI 207.2R-07[3] still recommends the Schmidt's method for determining temperature gradients. The method presented by Schmidt in 1924 allows solving the heat conduction problem by a simple averaging process which can often be done by hand or by graphical constructions[4]. In essence, it is not more than an old-fashioned usage of finite difference explicit formulation.

Somewhere between those two quite opposite approaches, several models have been proposed in recent years in order to study the early-age behaviour of massive concrete structures by means of finite element calculations. Ishikawa[5] and Luna and Wu[6] addressed the problem of computing the heat of hydration using an exponential function

[†] Former MSc student at Instituto Superior Técnico, University of Lisbon.
[‡] Instituto Superior Técnico, University of Lisbon.

of time to represent the adiabatic temperature rise. Cervera et al.[7], Lackner and Mang[8] and Fairbairn et al.[9], among others, use a more sophisticated formulation written in the framework of thermodynamics of chemically reactive porous media based in the model presented by Ulm and Coussy[10].

This paper uses the methodology originally developed in Cervera et al. [11], in order to model the temperature distribution of Alqueva dam during construction. In the absence of specific adiabatic calorimetric tests of the concrete mixes used in Alqueva, an exponential function was calibrated by the best fitting of estimated heat of hydration at the ages of 3, 7 and 28 days. The predicted temperatures obtained from the code are compared with the actual temperatures measured in situ by the monitoring system installed in the dam.

2 CHEMO-THERMAL MODEL

2.1 Evolution of the hydration reaction

The Ulm and Coussy's model[10] considers concrete as a reactive porous media composed of a solid skeleton of anhydrous cement grains, calcium silicate hydrates (CSH) and pores that may be filled by either air or water. Within this framework, the hydration process of concrete can be viewed, from a macroscopic level, as a chemical reaction in which the free water is a reactant phase that combines with the unhydrated cement to form combined water in the hydrates as a product phase. This implies that the micro-diffusion of water through the layers of already formed hydrates can be considered as dominant mechanism in the kinetics of the reaction[11].

The evolution of the hydration reaction is represented by an Arrhenius-type equation, which takes into account the thermo-activation and exothermic nature of the reaction[12]:

$$\frac{\mathrm{d}m}{\mathrm{d}t} = \frac{1}{\eta} A \exp\left(-\frac{E_\mathrm{a}}{RT}\right) \tag{1}$$

where dm/dt is the variation of the skeleton mass (reaction velocity); η is a viscosity term representing the increase in physical barrier of CSH, which tends to isolate the cement grain from the free water and depends on the state of hydration reaction; A is the affinity of the chemical reaction or, in other words, the thermodynamic force associated to the rate of hydration formation, which also depends on the state of the hydration reaction; E_a is the apparent thermal activation energy, which is considered to be constant with relation to the hydration degree; R is the universal constant of gases; and T is the temperature in Kelvin.

For practical purpose, it is convenient to rewrite the model in terms of the normalized variable called hydration degree, defined as the relation between the mass of the skeleton at time t normalized by the mass of the skeleton when hydration is complete, i.e., $\xi(t) = m(t)/m_\infty$:

$$\dot{\xi} = \tilde{A}(\xi) \exp\left(-\frac{E_\mathrm{a}}{RT}\right) \tag{2}$$

where $\dot{\xi}$ is the time derivative of ξ. The function $\tilde{A}(\xi) = A/\eta$ is the normalized affinity which completely characterizes the macroscopic hydration kinetics for a given concrete mixture. To represent $\tilde{A}(\xi)$ Cervera et al. proposed the following analytical expression:

$$\tilde{A}(\xi) = \frac{k_\xi}{\eta_{\xi o}}\left(\frac{A_{\xi o}}{k_\xi \xi_\infty} + \xi\right)(\xi_\infty - \xi)\,\exp\left(-\overline{\eta}\,\frac{\xi}{\xi_\infty}\right) \tag{3}$$

where k_∞, $A_{\xi o}$, $\eta_{\xi o}$ and $\overline{\eta}$ are material properties and ξ_∞ is the asymptotic degree of hydration, which has been shown to be always smaller than the unity[13].

2.2 Thermo-chemical coupling

The problem of heat transfer during concrete hydration is obtained from the classical heat equation by including the term $L\dot{\xi}$ representing the heat generated by the exothermic reaction:

$$k\nabla^2 T + G + L\dot{\xi} = \rho c\dot{T} \tag{4}$$

were k is the thermal conductivity, ρ is the density, c is the specific heat, G are the external volumetric heat sources and L is the latent heat of hydration.

The solution of equation (4) together with equation (2) represents the thermo-chemical coupling and constitutes a nonlinear problem in T and ξ.

The thermal model description is completed by stating boundary conditions and initial conditions.

3 DETERMINATION OF THE HEAT OF HYDRATION

According to Cervera et al.[11] the material properties involved in expression (3) can be determined experimentally by an adiabatic calorimetric test considering:

$$\tilde{A}(\xi) = \frac{\xi_\infty \dot{T}^{ad}}{T_\infty^{ad} - T_o}\exp\left(\frac{E_a}{RT}\right) \tag{5}$$

and

$$\xi = \xi_\infty \frac{T^{ad} - T_o}{T_\infty^{ad} - T_o} \tag{6}$$

where T^{ad} is the measured temperature along the experiment, $\dot{T}^{ad}$ is the measured temperature rate, T_∞^{ad} is the final reached temperature and T_o is the initial temperature. The final degree of hydration ξ_∞ is related to the water/cement ratio of the mixture and can be estimated by:

$$\xi_\infty = \frac{1.031 w/c}{0.194 + w/c} \tag{7}$$

However, in many cases, the available data of heat of hydration is usually restricted to a few points. Thus, in order to represent the whole course of the adiabatic hydration process, an analytical expression have to be fitted to the data points. For example, adopting the function[14]:

$$Q = a\exp\left(\frac{b}{t}\right) \tag{8}$$

with $a = Q_\infty$ and b determined by linear regression, the adiabatic temperature rise can be expressed as:

$$T^{ad} = \frac{a}{c}\exp\left(\frac{b}{t}\right) \tag{9}$$

and the normalized affinity functions (5) results:

$$\tilde{A}(\xi) = \frac{\xi_\infty}{T_\infty^{ad} - T_o}\exp\left(\frac{E_a}{RT}\right) a\,b\,\exp\left(\frac{b}{t}\right)\frac{1}{ct^2} \tag{10}$$

Finally, the analytical expression (3) is determined by calibrating the three material properties $k_\xi/\eta_{\xi o}$, $A_{\xi o}/k_\xi$ and $\overline{\eta}$ with expression (10).

4 APLICATION TO ALQUEVA DAM

4.1 Project description

Alqueva dam creates the largest artificial lake in Western Europe, with storage capacity of 4150 hm^3 and a surface area of 250 km^2 at the retention water level. The dam is located on the River Guadiana, in the south-east of Portugal, and is the main structure of a multipurpose development designed for irrigation, energy production and water supply. It is a double curvature arch dam, with a maximum height of 96 m and a total length of 348 m between the abutments at the crest elevation (154 m). The dam width is 7 m at the crest, while at the base it varies from 30 m at the central cantilever to 33 m at the abutments. The powerhouse is located at the toe of the dam with a dam-wall downstream.

4.2 Finite Element Model

The mesh of the dam comprises four layers of 20 nodes solid elements through its thickness and two elements in the width of each block. The vertical thickness of the elements varies from 2 to 3 m in order to represent the concrete placing lift. A total of 18,857 elements were used to model the dam including its foundation.

The transient thermal analysis was performed with an in-house code which applies an implicit Euler backward finite difference scheme for the time discretization and a finite element scheme for the spatial discretization.

The finite element model of the dam was updated for every construction stage by applying the birth and death method. In order to deal with the birth of the 11,328 elements representing the dam and to update the boundary conditions, a specific program was implemented.

4.3 Material properties

Table 1 summarized the material properties used in the analysis.

Properties	***Rock mass foundation***	***Concrete***
density ρ [kg/m^3]	2600	2400
specific heat c [J/(kg K)]	879	920
thermal conductivity k [W/(m K)]	4.6	2.62
absorption coefficient a	0	0.65

Table 1: Material properties.

As part of the *Concrete Quality Assurance*[15], 98 samples of cement were tested to determine the heat of hydration at the age of 3, 7 and 28 days. The average results reported in this document are given in table 2.

Age [days]	***Q*** [kJ/kg]
3	242
7	271
28	291

Table 2: Cement heat of hydration.

Applying the approach given in point 3 to an average composition concrete characterized by a content of cement of 160 kg per cubic meter of concrete and a ratio w/c = 0.49, the following heat of hydration characteristics were determined:

$$Q = 19.4 \exp\left(\frac{-12.8}{t}\right) \tag{11}$$

$$\xi_\infty = 0.74 \quad ; \quad k_\xi / \eta_{\xi o} = 555 \text{s}^{-1} \quad ; \quad A_{\xi o} / k_\xi = 0.0015 \quad ; \quad \overline{\eta} = 5.47 \tag{12}$$

The adiabatic temperature rise and the normalized affinity obtained are illustrated in figure 1. Figure 1(a) shows the comparison between the estimated values of heat of hydration at the age of 3, 7 and 28 days and the equation (11). Figure 1(b) shows the comparison of the estimated normalized affinity based on the derivative of equation (11) and the Cervera's analytical expression (3) evaluated with the parameters shown in (12).

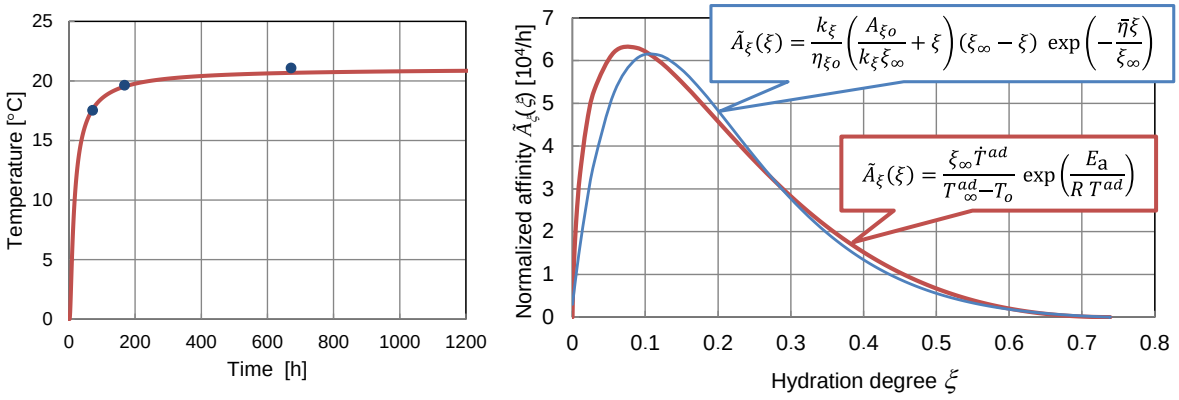

(a) (b)

Figure 1: (a) Comparison of estimated values (data points) and simulated (solid line) adiabatic temperature rise; (b) Comparison of simulated normalized affinity and Cervera's analytical expression

4.4 Boundary and initial conditions

Convection/radiation heat transfer and solar radiation flux absorption boundary conditions were applied in all air-exposed boundaries. Adiabatic boundary conditions were applied at the lateral and bottom boundary of the rock mass foundation and at the inner surfaces of the water intakes and the spillways orifices.

The total thermal transmission coefficient was estimated based on average wind conditions. A constant value h_t = 20.2 W/(m^2 K) was applied to the whole model, except in the surfaces insulated by the formwork, where the transmission coefficient was reduced to h_t = 2.02 W/(m^2 K).

In order to simulate the construction phase, the boundary conditions had to be updated at every construction stage. Figure 2 illustrates the mesh of the dam in July 24, 2000, where air-exposed faces are indicated in blue, faces with formwork in green, and faces with adiabatic boundary conditions in red. A photo showing the same stage is also included for comparison.

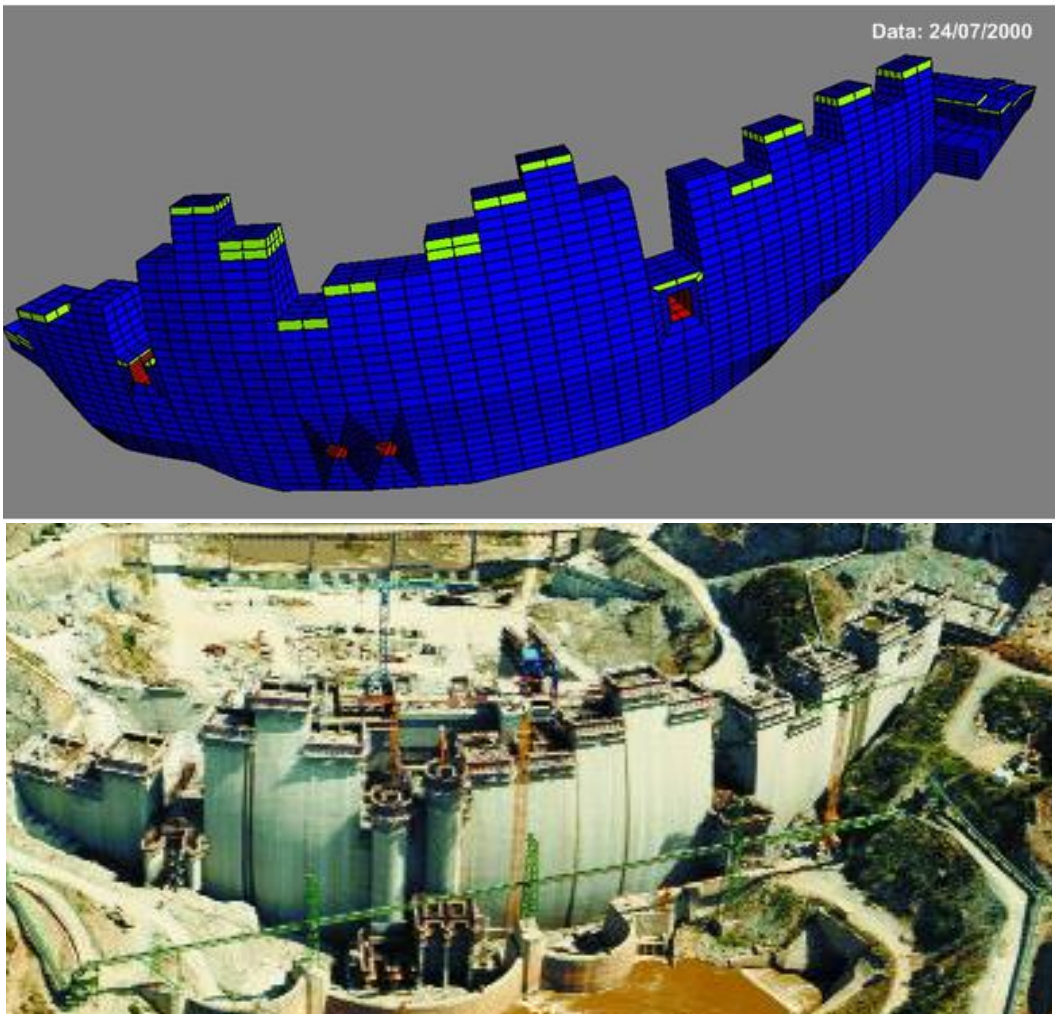

Figure 2: Construction phase simulation

The daily temperature variation was modelled by cosine functions based on field air temperature measurements.

To calculate the solar irradiance, the radiative model reporter by Kumar[16] was implemented. This model is based on older ones (Kreith and Kreider[17] and Liu and Jordan[18]) and provides the backbone for the Solrad and Shortwave routines of the ArcInfo GIS which was developed for GIS applications in agriculture and ecology[19]. A detailed description of its implantation can be found in Castilho[20].

To start the construction phase, a previous thermal analysis was carried out considering only the foundation. After achieving convergence, the computed results were applied as initial temperatures at foundation nodes.

Air temperature was adopted as the initial concrete temperature at the time of placement. When the air temperature exceeded the limiting placing temperature of 7°C and 25°C, the temperature was fixed to the corresponding limit.

4.5 Results

Comparisons of the temperatures obtained by the finite element simulation with the observed temperatures are shown in figures 3-5. It is worth noting that since year 2001 the cooling of the concrete by piped water was applied in stepwise progression starting from the bottom. The objective of this post-cooling was to broaden the openings of the contractions joint to facilitate their grouting. As the thermal code does not model the cooling of concrete by piped water, it was not possible to simulate the evolution of the temperature from that stage.

Figures 3 and 4 compare the evolution between the observed and calculated temperatures for points located in the middle of block 8-9 and 13-14, respectively. Both blocks have the same cross section with a height of 96 m. Through the examination of both figures it is possible to note that, in general, there is a very good agreement between the observed values and the computed temperature up to the time when the post-cooling was applied. The differences observed in extensometer G2 and thermometer T32 is assumed to be originated from the differences between the real and the adopted placing temperature. It is worth noting the important role played by the placement temperature by comparing G2 with G5 and T19 with T32. It is also interesting to observe the influence of the seasonal variation of the air temperature in points near the dam surfaces, as in thermometers T59 and T64.

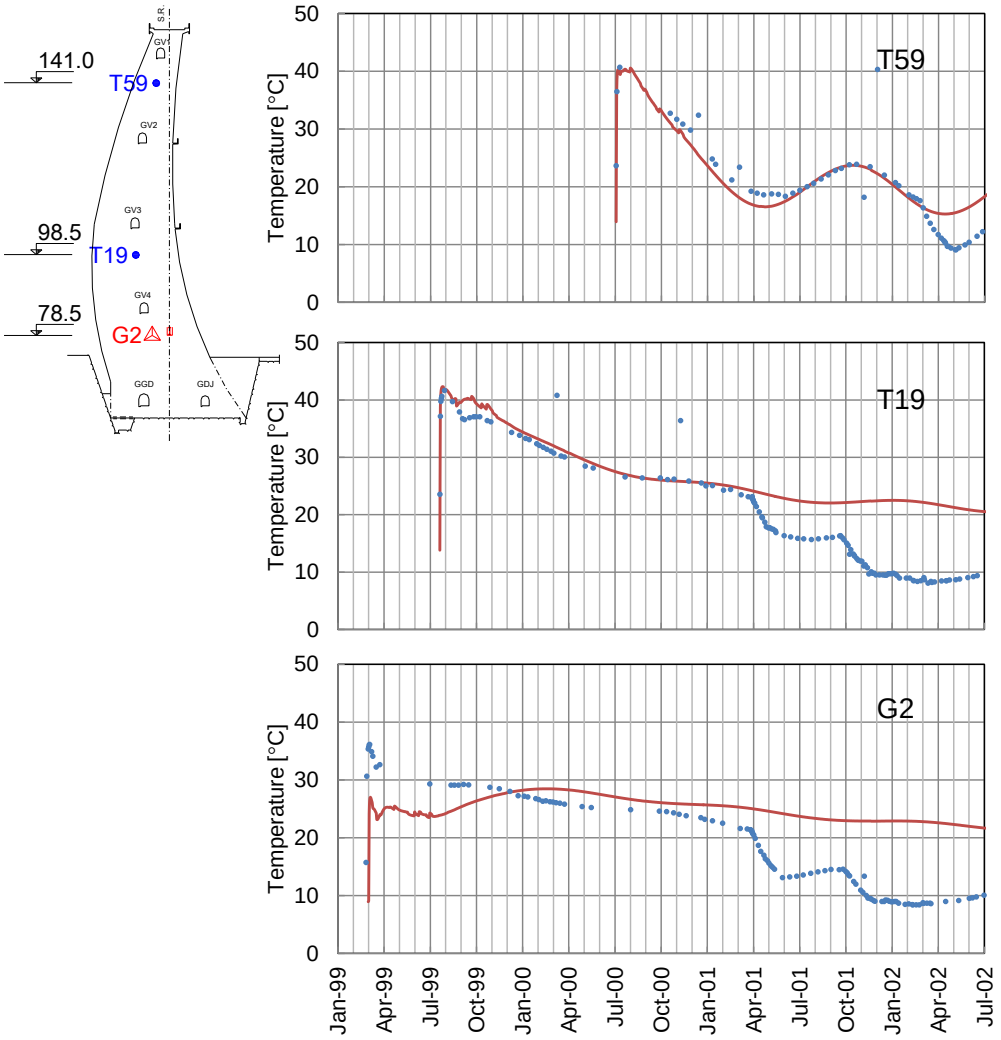

Figure 3: Comparison of observed values (data points) and simulated (solid line) temperature evolution inside block 8-9.

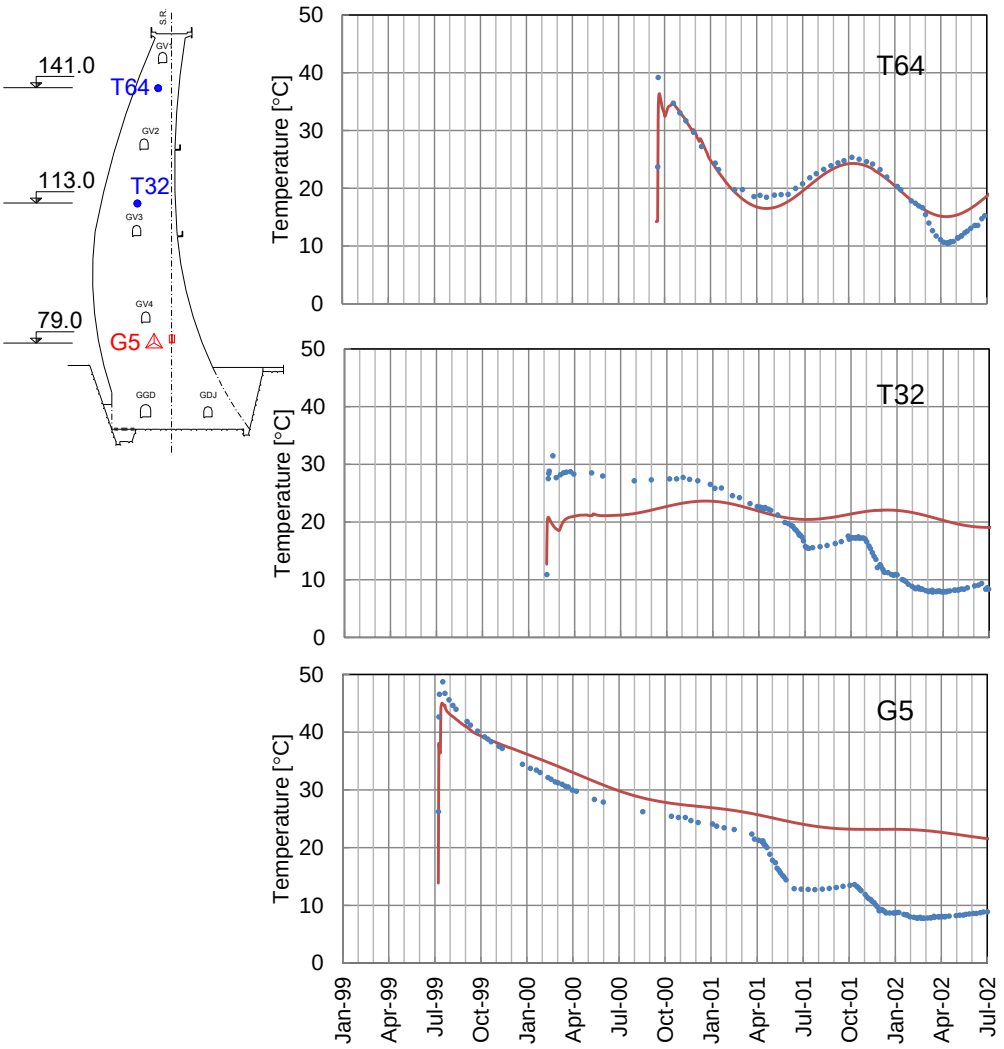

Figure 4: Comparison of observed values (data points) and simulated (solid line) temperature evolution inside block 13-14.

Figure 5 shows the evolution of temperature in points on the faces of the dam. Although the analysis was conducted considering an incremental time of 1 h, only the temperature obtained once a day was represented, i.e. thus excluding daily variations. In both cases the heat of hydration was dissipated in a short period of time given place to a seasonal fluctuation following the air temperature. The values observed in the downstream face exhibit greater dispersion than the values recorded in the upstream face due to the different exposure to solar radiation.

5 CONCLUSIONS

The application of a thermo-chemical model to the analysis of the temperature distribution of Alqueva dam during construction has been investigated in this work.

The adiabatic temperature rise of the concrete was represented by an exponential function obtained by the best fitting of estimated heat of hydration at the ages of 3, 7 and 28 days.

The finite element code used in this study has been shown to provide good quality simulations of the thermal response of Alqueva dam during construction.

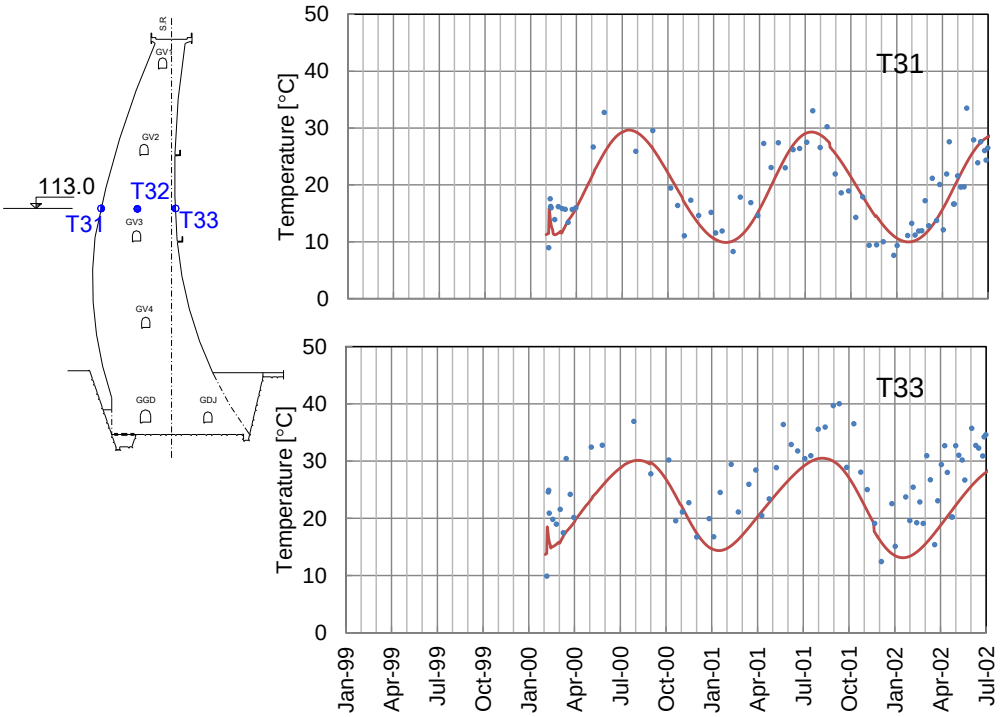

Figure 5: Comparison of observed values (data points) and simulated (solid line) temperature evolution in the dam faces at block 13-14.

AKNOWLEDGEMENT

The permission of EDIA- Empresa de Desenvolvimento de Infraestruturas de Alqueva, S.A. to use the data related to Alqueva dam is acknowledged.

REFERENCES

[1] A. Malkawi, S. Mutasher and T. Qiu, "Thermal-structural modeling and temperature control of roller compacted concrete gravity dam", *J Performance of Constructed Facilities*, ASCE, 17(4), 177-187, (2003).

[2] V.Smilauer and T. Krejci, "Multiscale model for temperature distribution in hydrating concrete", *Int. J. Multiscale Engineering*, 7(2), 135-151, (2009).

[3] 207.2R-07, *Report on thermal and volume change effects on cracking of mass concrete*, American Concrete Institute, (2007).

[4] G. Dusinberre, *Numerical analysis of heat flow*, McGraw-Hill Book Company, Inc., (1949).

[5] M. Ishikawa, "Thermal stress analysis of a concrete dam", *Computers & Structures*, 40(2), 347-352, (1991).

[6] R. Luna and Y. Wu, "Simulation of temperature and stress fields during RCC dam construction*", J. Construction Engineering and Management*, 126(5), (2000).

[7] M. Cervera, J. Oliver and T. Prato, "Simulation of construction of RCC dams. I:

Temperature and aging", *J. Structural Engineering*, ASCE, 126(9), 1053-1061, (2000).

[8] R. Lackner and H. Mang, "Chemoplastic material model for the simulation of early-age cracking: From the constitutive law to numerical analyses of massive concrete structures", *Cement & Concrete Composites*, 26, 551-562, (2004).

[9] E. Fairbairn, I. Ferreira, G. Cordeiro, M.Silvoso, R. Toledo Filho and F. Ribeiro, "Numerical simulation of dam construction using low-CO_2 emission concrete", J. *Material and Structures*, RILEM, (2009).

[10] F.J. Ulm and O. Coussy, "Modeling of thermochemomechanical couplings of concrete at early ages". *J. Engrg. Mech.*, ASCE, 121(7), 185-794, (1995).

[11] M. Cervera, J. Oliver and T. Prato, "Thermo-chemo-mechanical model for concrete. I: Hydration and aging". *J. Engrg. Mech.*, ASCE, 125(97), 1018-1027, (1999).

[12] M. Silvoso, *Numerical modeling of concrete at early-ages*. M.Sc. thesis, COPPE/The Federal University of Rio de Janeiro, Rio de Janeiro, Brazil, (2002) (in Portuguese).

[13] G. Di Luzio and G. Cusatis, "Hygro-thermal-chemical modeling of high performance concrete. I: Theory", *Cement & Concrete Composites*, 31, 301-308, (2009).

[14] L.G. Silva, *Caracterização das propriedades termo-mecânicas do betão nas primeiras idades para aplicação estrutural*. M.Sc. thesis, FEUP, Porto University, Porto, Portugal, (2007) (in Portuguese).

[15] LNEC, *Apreciação sobre o controlo da qualidade do betão aplicado na barragem do Alqueva - relatório final*, Relatório 106/2003 DM, (2003) (in Portuguese).

[16] L. Kumar, A. Skidmore and E. Knowles, "Modelling topographic variation in solar radiation in a GIS environment", *Int. J. Geographical Information Science*, 11(5), 475-497, (1997).

[17] F. Kreith and J. Kreider, *Principles of solar engineering*, Hemisphere Publishing Corporation, (1978).

[18] B. Liu and R. Jordan, "The interrelationship and characteristic distribution of direct, diffuse and total solar radiation", *Solar Energy*, 4(3), 1-19, (1960).

[19] C. Gueymard, "Clear-sky irradiance predictions for solar resource mapping and large-scale applications: Improved validation methodology and detailed performance analysis of 18 broadband radiative models", *Solar Energy*, 86, (2012).

[20] E. Castilho dos Santos. *Análise térmica de barragens de betão durante a construção. Aplicação à barragem de Alqueva*. M.Sc. thesis, Instituto Superior Técnico, University of Lisbon, Lisbon, Portugal, (2013) (in Portuguese).

Castilho, E.; Leitão, N.S.; Tiago, C. (2015) – "Thermal analysis of concrete dams during construction phase". Dam World Conference, Lisboa, abril 21-24 2015.

ERRATA

Página	*Localização*	*Onde se lê*	*Deve ler-se*
4	Eq. (9)	$T^{ad} = \frac{a}{c}\exp\left(\frac{b}{t}\right)$	$T^{ad} = \frac{a}{\rho c}\exp\left(\frac{b}{t}\right)$
4	Eq. (10)	$\tilde{A}(\xi) = \frac{\xi_\infty}{T_\infty^{ad} - T_o}\exp\left(\frac{E_a}{RT}\right)$ $a\,b\,\exp\left(\frac{b}{t}\right)\frac{1}{ct^2}$	$\tilde{A}(\xi) = \frac{\xi_\infty}{T_\infty^{ad} - T_o}\exp\left(\frac{E_a}{RT}\right)$ $\left[-a\,b\,\exp\left(\frac{b}{t}\right)\frac{1}{\rho c t^2}\right]$